N89-10854

AN ASSESSMENT OF GROUND EFFECTS DETERMINED BY STATIC AND

DYNAMIC TESTING TECHNIQUES

John W. Paulson, Jr.

Guy T. Kemmerly

NASA Langley Research Center
Hampton, Virginia 23665

PRECEDING PAGE BLANK NOT FILMED

INTRODUCTION

Historically, aircraft ground effects have been determined by placing a model configuration in the wind tunnel, obtaining data at various heights above a ground plane and analyzing the results as a function of height. This approach yields time averaged static aerodynamic data as a function of height above the ground plane for use in analyzing aircraft performance during approach and landing. In actual flight testing ground effects can be determined in two ways: constant altitude flight above the ground, or descending flight toward the ground (final approach and landing)-both conducted at constant air speed and angle-of-attack. Results obtained with the constant altitude flight method and conventional wind tunnel ground effects tests are generally in good agreement (refs. 1-3). That is, lift increases, drag decreases and pitching moment changes indicated in static wind tunnel data are found to be present in flight results. However, if the flight test is conducted as a landing approach, where aircraft height varies with time as a function of rate of descent, then the flight test and wind tunnel results are not always in agreement (refs. 4-5). In particular, the increase in lift coefficient as the ground plane is approached seems to be lower when the aircraft has a rate-of-descent as compared to the case where rate-of-descent is zero or to static wind tunnel results. This variation in results appears to be caused by differences in the interactions that occur between the trailing vortex/wake system and ground plane (fig. 1) during descending flight ($\gamma < 0°$) and during level flight or static wind-tunnel tests ($\gamma = 0°$). These results have led to the hypothesis that rate-of-descent could be an important parameter in determining ground effects. The effects of sink rate might be particularly pronounced if vectored or reversed exhaust flows are involved,

122

I

which greatly amplifies the interactions of the exhaust, freestream, and the ground plane. In the past, the aircraft rate-of-descent has been simulated during wind-tunnel testing by moving the model vertically in the wind tunnel toward a ground plane. This method, described in references 6-7, was developed at Kansas University. Research conducted using the technique showed that a configuration with a rate-of-descent of up to about 3 ft/sec experienced less increase in lift in ground effect compared to static wind tunnel results at constant heights. However, this method is somewhat limited in maximum rate-of-descent because of the accelerations and vertical velocities possible within the confines of closed wind-tunnel test sections.

The present study was undertaken to evaluate the use of a new dynamic ground effects testing technique wherein a model is moved horizontally over an inclined ground plane. The evaluation was conducted at the Langley Research Center utilizing the Langley Vortex Research Facility (VRF). During the tests, the model is carried horizontally by a motorized cart down a towing tank at velocities up to 100 ft/sec and approaches a 4° inclined ground board producing effective descent rates of up to about 7 ft/sec. The VRF facility provides extensive data acquisition and support equipment, including compressed air for exhaust flow simulations. The study included the development of the dynamic test technique in the VRF and conventional ground effects tests in the Langley Research Center 14- by 22-Foot Subsonic Tunnel. These tests, using the same models and sting support hardware, allowed for a direct comparison between static and dynamic procedures to assess the effect of rate-of-descent on ground effect testing results. A description of the testing techniques and sample results are the subjects of this paper.

SYMBOLS

b	wing span, ft.
C_L	lift coefficient, Lift/ $q_\infty S$
ΔC_L	percent change in lift coefficient $(C_{L_{IGE}} - C_{L_{OGE}})/C_{L_{OGE}}$
d/dt	derivative with respect to time
g	acceleration due to gravity, 32.2 ft/sec^2
h	height above ground plane, ft.
$\dot{h}$	rate-of-descent, dh/dt, ft/sec.
NPR	nozzle total pressure ratio, P_t/P
P_t	nozzle total pressure, lbf/ft^2
P	static pressure, lbf/ft^2
q_∞	dynamic pressure, 1/2 ρV^2 , lbf/ft^2
S	wing area, ft^2
t	time, sec.
V	velocity, ft/sec.
α	angle-of-attack, deg.
γ	flight path angle, deg.
δ	deflection angle, deg.
θ	pitch attitude, deg.
ρ	density, slugs/ft^3

Subscripts:

IGE	in ground effect
OGE	out of ground effect
∞	freestream conditions
j	exhaust jet conditions

TEST TECHNIQUES AND MODEL HARDWARE

To produce a rate-of-descent in a ground based facility the model must effectively move toward a simulated ground plane. In the Vortex Research Facility (VRF) this was accomplished by moving the model horizontally over a ground board inclined toward the model path as shown in figures 2 and 3. In this procedure, the combination of forward velocity and ground board angle produced a rate-of-descent ($\dot{h}$) equal to $V_\infty \tan 4°$ where V_∞ was varied up to 100 ft/sec, resulting in values of $\dot{h}$ up to 7 ft/sec.

In the VRF the sting-mounted models were attached to a vertical blade support system suspended below a powered cart which travels on rails above the test section (fig. 4). The cart was powered by a high-performance automobile engine and included electrical, mechanical and high-pressure air systems which provided data acquisition, control of test conditions and model/cart safety. Prior to a typical run, angle-of-attack and minimum ground height were preset using the support hardware. The cart accelerated up to the desired test velocity, which was maintained by a normal automobile cruise control system. The 14-foot high by 17-foot wide by 600-foot long test section shielded the model from the bow wave created by the moving cart. Before the test section was entered, air valves opened which allowed time for the exhaust flow to be stabilized at a desired nozzle pressure ratio before the model approached the ground board. As the model passed over the 100-foot long ramp section of the ground board, the height of the model over the ground board decreased to a minimum h/b which then remained constant over the 50 foot long flat portion of the ground board. Thus, during a single data run both dynamic (time varying height) and steady state (constant height) data were obtained. The data obtained consisted of aerodynamic forces and moments measured on a 6-component

balance, high pressure air data for exhaust flow characteristics, and cart velocity for test conditions. In addition, model and sting accelerations were recorded in order to remove inertial loads from the balance output. At the test section exit, the cart engine was shutdown and brakes were applied which brought the cart to rest with a 2-g decelaration. Because of this deceleration, the model had to be kept as light as possible (i.e. less than 25 lb.) to prevent the balance size from becoming so large that the low aerodynamic forces could not be measured accurately.

The models used in this investigation were the flat plate 60° delta wing (b = 3 ft.) shown in figure 5, and the 7-percent scale F-18 configuration shown in figure 6. Both models were equipped with non-metric reversed-thrust nozzles: The 60° delta wing used simple convergent pipes bent to 45° and the F-18 used a modification of a reverse nozzle/plenum box from a previous generic thrust reverser program (ref. 8). Both models were tested at various forward velocities (and hence rates-of-descent), minimum ground heights, nozzle pressure ratios and angles-of-attack in the VRF, and the resulting dynamic- and steady-state ground effects were determined for the unpowered and reverse thrust cases. After the VRF tests were completed, the same model/sting/airline configurations were installed in the 14- by 22-Foot Subsonic Tunnel and the static ground effects were determined with and without the moving belt ground plane. In this wind tunnel, the tunnel floor boundary layer is always removed during ground effects testing by a vacuum system located at the test section entrance. This ensures that with or without the moving belt, there is initially no boundary layer on the test section floor. The models had been designed and fabricated to allow the same sting support to

|

be used in both facilities to minimize support interference and to permit the direct comparison of the differences between static, steady state and dynamic ground effects.

DISCUSSIONS

The following discussion presents the effect of the moving ground belt on static wind-tunnel ground effects for both unpowered and reversed thrust cases with the 60° delta wing. The static ground effect results are then compared with the dynamic and steady state results from the VRF for both the 60° delta and the F-18 configuration. Finally the dynamic results for the unpowered 60° delta wing are analyzed as a function of rate-of-descent.

Effect of Moving Belt. For years it has been known that the wind-tunnel floor boundary layer can affect the results obtained from static wind-tunnel ground effects testing. Twenty years ago, studies showed that moving the tunnel floor at the freestream velocity could eliminate this floor boundary layer and improve ground effect results. The research reported in reference 9 presented a boundary of C_L versus h/b which defined the need for using the moving belt during ground effects testing. Because of the high values of C_L and relatively low low values of h/b required before the moving belt was needed, it was assumed that conventional powered fighter configurations would not require the belt for testing. However, since current fighter concepts may utilize reverse thrust on approach, it was felt that during this dynamic ground effect study an examination should be made of the influence of the moving belt on ground effects.

As expected, the effect of the moving belt on the static ground effects of the unpowered 60° delta wing was essentially nill (fig. 7). However, when the

thrust reversers were employed for the delta wing (fig. 8) the moving belt

influenced the static ground effects. Since the reversed flow was penetrating

against relatively high-energy freestream air (rather than a boundary layer)

when the belt was moving, it did not flow as far forward and produced a lower

loss in lift at low ground heights as compared to the fixed floor results.

This trend was consistent for all configurations tested, and led to the

conclusion that the moving belt may be required for wind tunnel ground effects

testing of thrust-reversing configurations.

Comparison of Dynamic and Static Ground Effects. Since the magnitude of

the lift increase in ground effect for the unpowered 60° delta wing was small,

the comparison of static and dynamic ground effects is presented in figure 9

in terms of percent change in lift rather than lift coefficient. For a test

condition of V_∞ = 70 ft/sec, α = 10° and a sink rate of 4.9 ft/sec, the

percent increase in lift as the ground plane is approached was lower than that

produced from the static ground effects. As mentioned earlier, the change due

to sink rate is probably caused by differences in the interactions of the

model wake with the ground plane in dynamic and static conditions. Note that

the solid data point in figure 9 represents the steady state results from the

VRF where the model was traveling over the 50 foot long flat portion of the

ground board. These steady-state results compare well with those obtained

during the static tests in the wind tunnel.

The comparison between dynamic and static ground effect was more dramatic

when thrust reversers were employed on the 60° delta wing as shown in figure

10. These data indicate that the well-known loss in lift as the ground plane

was approached statically was not present at all in the dynamic case. In

fact, the model exhibited an increase in lift in the dynamic test. This

result was caused by the model effectively "running away" from the reversed

128

I

thrust plume. However, once the model passed over the flat ground board the reversed flow field had time to establish steady state conditions and the result was close to the static wind-tunnel ground effects. The test condition was set to simulate a jet to freestream dynamic pressure ratio of approximately 100 which is representative of normal approach power setting for a fighter aircraft. If the dynamic pressure ratio were increased (i.e. the throttle setting advanced or the approach velocity reduced), then the reverse flow plume would be expected to penetrate farther forward and the ground effects would probably be different than the NPR = 1.6 case. The data shown in figure 11 for NPR = 1.8 indicate that the effect of the belt was reduced, and that the lift loss present in the static results was beginning to occur in the dynamic results as the reverse flow plume penetrated farther below and ahead of the model to interact with the ground plane at a greater distance than the lower NPR case. In effect, at this higher dynamic pressure ratio the model could not "escape" from the exhaust plume as the ground plane was approached. Once again, the steady state result was close to the static results.

Similar trends are shown for the F-18 configuration in figure 12 for a typical landing dynamic pressure ratio. It should be noted that the expected lift loss in the static data was of lower magnitude than the loss for the 60° delta wing. The F-18 exhaust nozzles were not located near the wing, but rather at the aft end of the fuselage and, therefore, have less effect on the wing flow field. However, this loss in lift was not indicated in the dynamic data and the steady state results matched the static results. As an assessment of on the effect of dynamic pressure ratio, the NPR was increased to 2.5 which yielded a dynamic pressure ratio much greater than a normal

approach condition. In this case, the plume should have been blown quite far ahead of and below the model. The data of figure 13 showed that the dynamic, static and steady state results were all similar indicating that the plume was in front of the model for all testing techniques.

Effect of Rate-of-Descent. In the VRF tests rate-of-descent could be varied by changing the cart velocity; unfortunately, this also changed test Reynolds number and dynamic pressure ratio. Since the 60° delta wing had a sharp leading edge, it was anticipated that Reynolds number effects would be small and that if the model was unpowered, a consistent set of data could be obtained at various rates-of-descent. Results presented in figure 14 show that increasing the rate-of-descent reduced the effect of the ground plane, resulting in reduced increases in lift at higher $\dot{h}$. This trend seems reasonable since at very high $\dot{h}$ an aircraft would be on the ground before the effect would be established.

CONCLUDING REMARKS

A new testing technique has been developed wherein rate of descent can be included as a parameter in ground effects investigations. This technique simulates rate of descent by horizontal motion of a model over an inclined ground board in the Langley Vortex Research Facility. During initial evaluations of the technique, dynamic ground effects data were obtained over the inclined ground board, steady state ground effects data were obtained over a flat portion of the ground board, and the results have been compared to conventional static wind tunnel ground effect data both with and without a moving belt ground plane simulation. Initial testing and analysis have led to the following conclusions:

130

|

1.) The moving belt ground plane had little effect on static ground effects for the configurations tested unless thrust reversers were employed. When thrust reversers were simulated, the moving belt yielded reduced lift losses in ground effect as the reversed nozzle flow could not penetrate against freestream flow as well as against the tunnel boundary layer.

2.) The inclusion of rate-of-descent in ground effects testing can have a significant effect on the results. In general, rate-of-descent reduced ground effects, compared to static or steady state results, to the point that for reversed thrust cases, an expected loss of lift due to ground effects was eliminated at approach conditions.

3.) In general, the the steady state results from the VRF matched static results obtained from the wind tunnel once the flow field stabilized over the flat portion of the ground board.

<div align="center">REFERENCES</div>

1. Pelagatti, C.; Pilon, J. C.; and Bardaud, J.: Analyse Critique des Comparaisons des Resultats de Vol aux Previsions de Soufflerie pour des Avions de Transport Subsonique et Supersonique. Paper 23, AGARD CP-187, Flight Ground Testing Facilities Correlation, 1975.

2. O'Leary, C. O.: Flight Measurements of Ground Effect on the List and Pitching Moment of a Large Transport Aircraft (Coment 3B) and Comparison with Wind Tunnel and Other Data. British ARC R&M 3611, June 1968.

3. Rolls, L. S.; and Koenig, D. G.: Flight-Measured Ground Effect on a Low-Aspect-Ratio Ogee Wing Including a Comparison with Wind-Tunnel Results. NASA TN D-3431, 1966.

4. Baker, P. A.; Schweikhard, W. G.; and Young, W. R.: Flight Evaluation of
   Ground Effect on Several Low-Aspect-Ratio Airplanes. NASA TN D-6053,
   October 1970.

5. Thomas, J. L.; Hassell, J. L.; and Nguyen, L. T.: Aerodynamic
   Characteristics in Ground Proximaty. Powered-Lift, Aerodynamics and
   Acoustics, Session I, Paper No. 9, Pg. 145, NASA SP-406, May 1976.

6. Chang, R. C.: An Experimental Investigation of Dynamic Ground Effect.
   KU-FRL-410-1, , Flight Research Laborartory, University of Kansas Center
   for Research, Incorporated, April 1985.

7. Lee, P. H.; Lan, C. E.; and Muirhead, V. U.: An Experimental
   Investigation of Dynamic Ground Effect. Prepared under NASA Grant NAG1-
   616, CRINC-FRL-717-1, Flight Research Laborartory, University of Kansas
   Center for Research, Incorporated, January 1987.

8. Joshi, P. B.: Generic Thrust Reverser Technology for Near Term
   Application. Volume 1-4, AFWAL-TR-84-3094, February 1985.

9. Turner, T. R.: A Moving-Belt Ground Plane for Wind-Tunnel Ground
   Simulation and Results for Two Jet-Flap Configurations. NASA TN D-4228,
   November 1967.

10. Turner, T. R.: Ground Influence on a Model Airfoil with a Jet-Augmented
    Flap as Determined by Two Techniques. NASA TN D-658, February 1961.

132

I

Normal approach

Steady state

$\alpha = 12°$ $\gamma = 0°$ $\theta = 12°$

$\dot{h} = 0$ ft/sec

Dynamic

$\alpha = 12°$ $\gamma = -5°$ $\theta = 7°$

$\dot{h} = \tan\gamma \cdot V_\infty$

Approach with thrust reverser
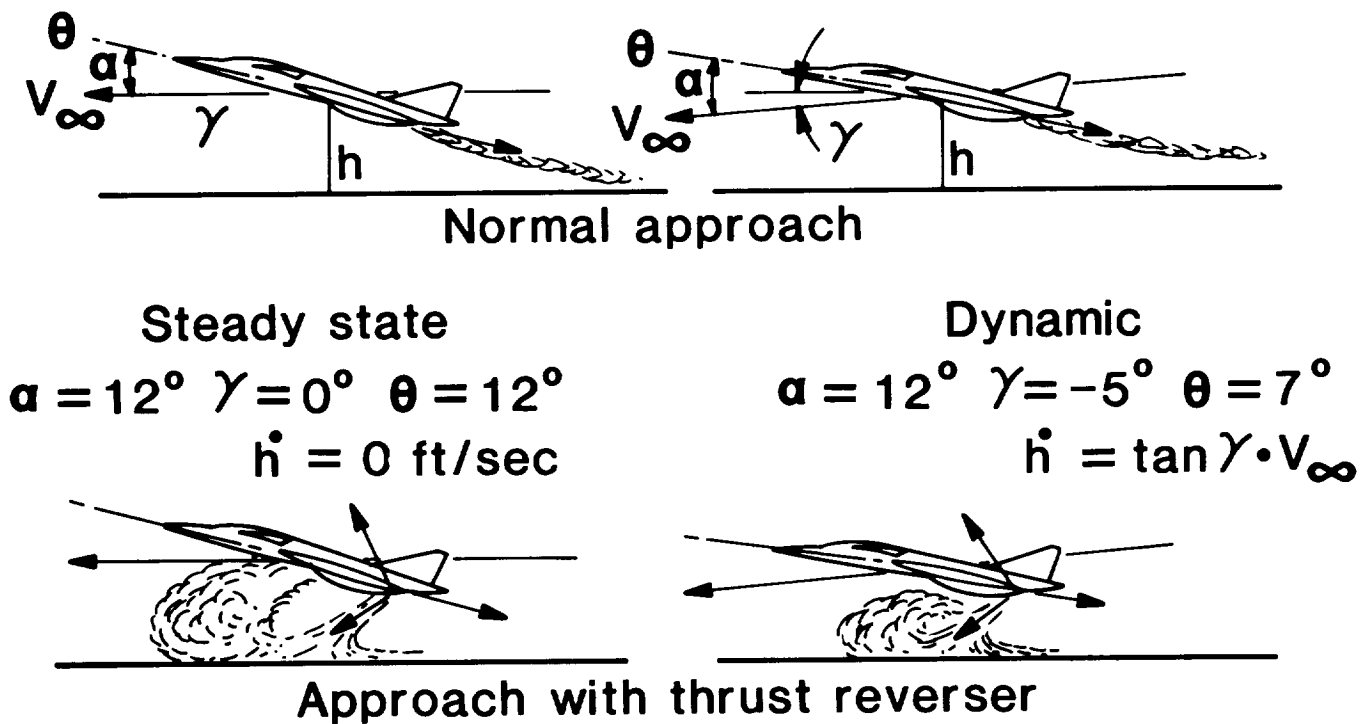
Figure 1. - Schematic of dynamic and steady state ground effects.
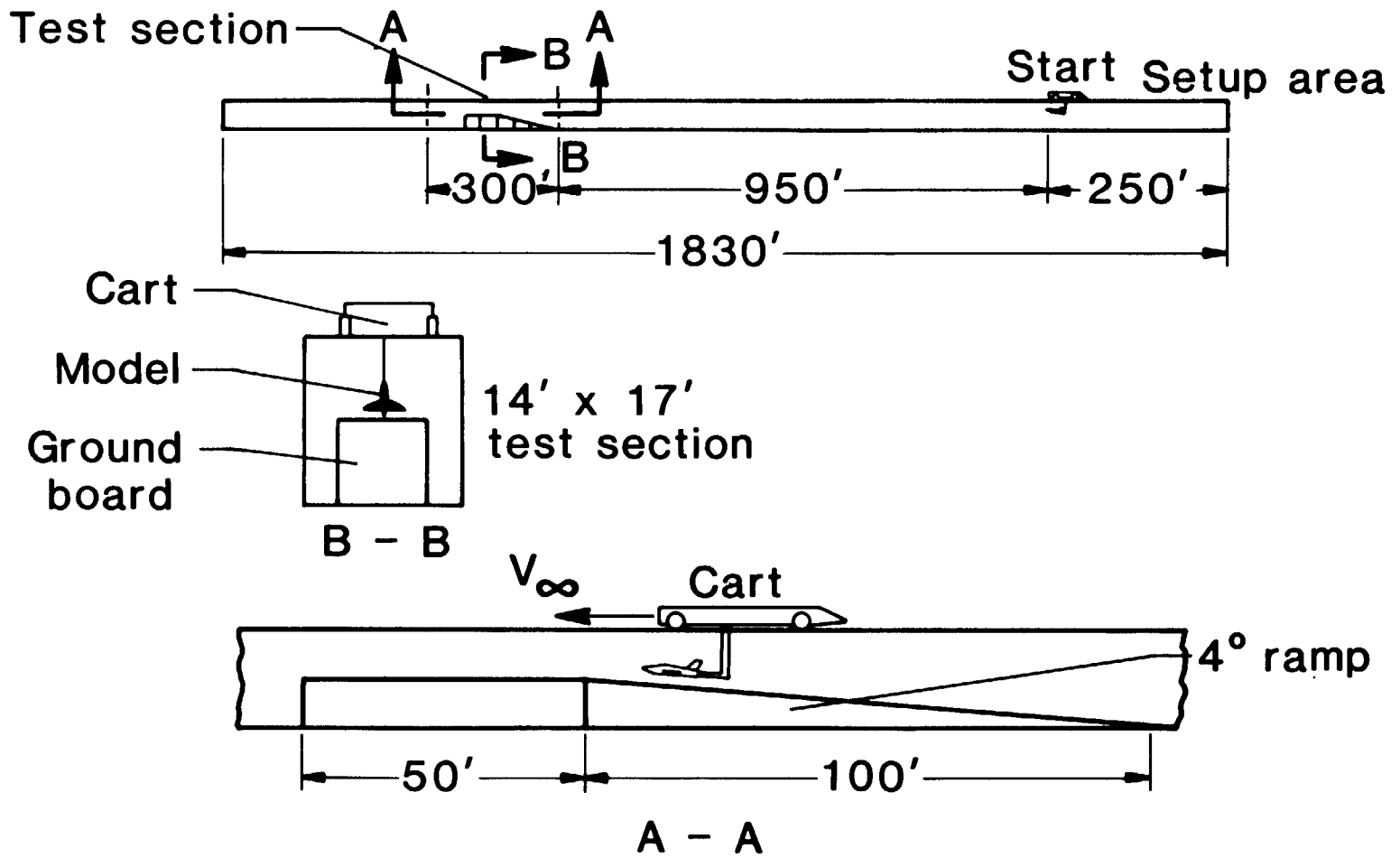
Figure 2. – Sketch of setup for dynamic ground effects testing in the Vortex Research Facility.

Support strut, sting,
high pressure airline
and instrumentation

Test section ceiling

V_∞ α

Ground board

Model path

h/b

γ

Test section floor
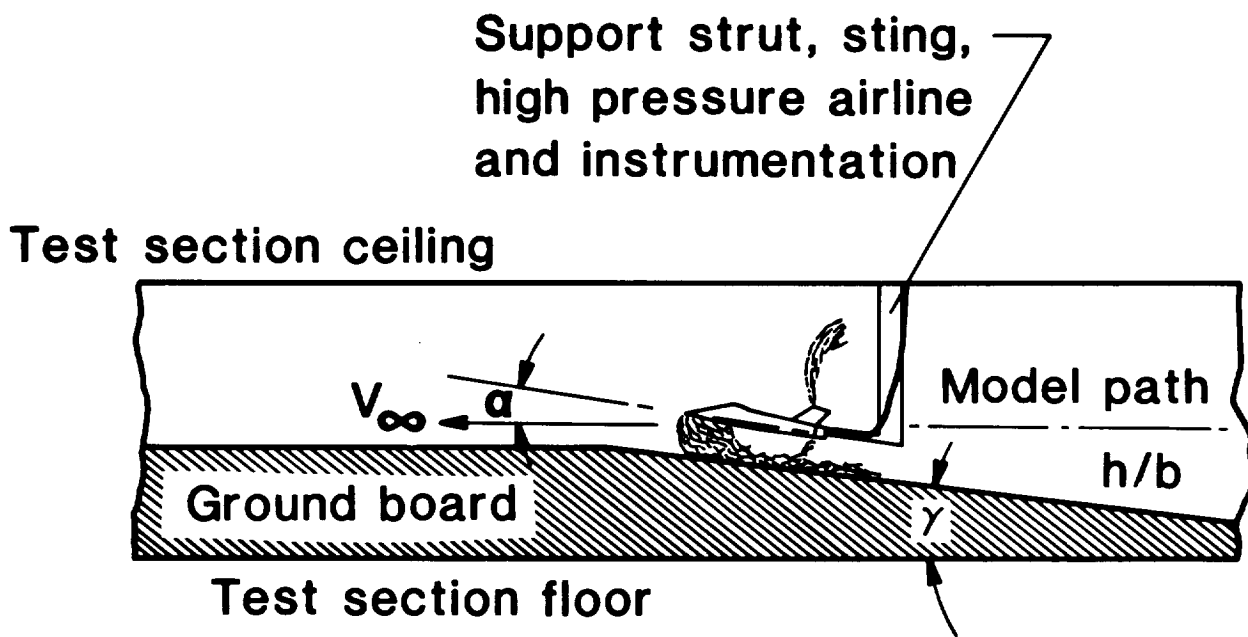
Figure 3. - Experimental concept in the Vortex Research Facility.

135
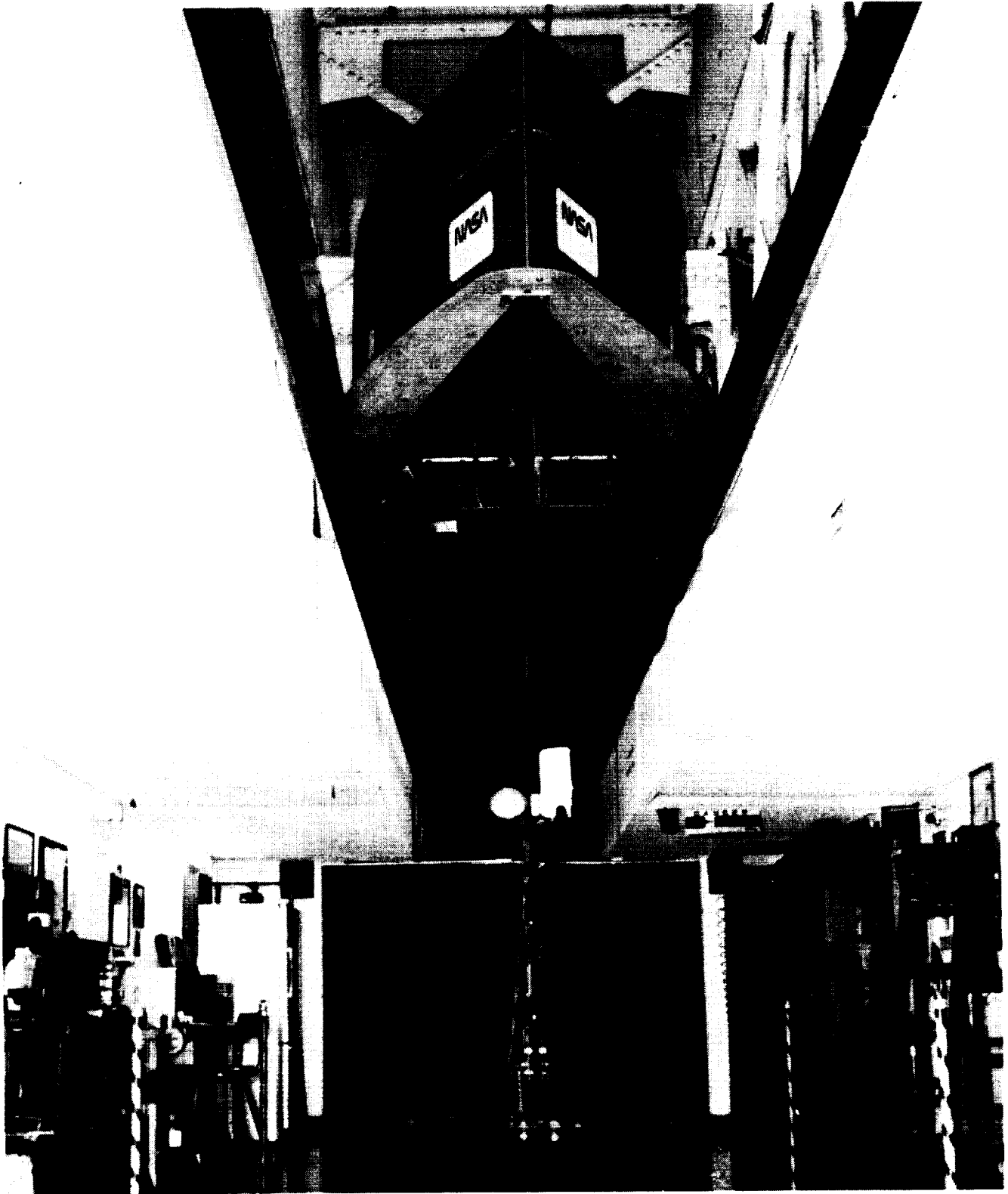
Figure 4. - Photograph of experimental setup in the Vortex Research Facility.
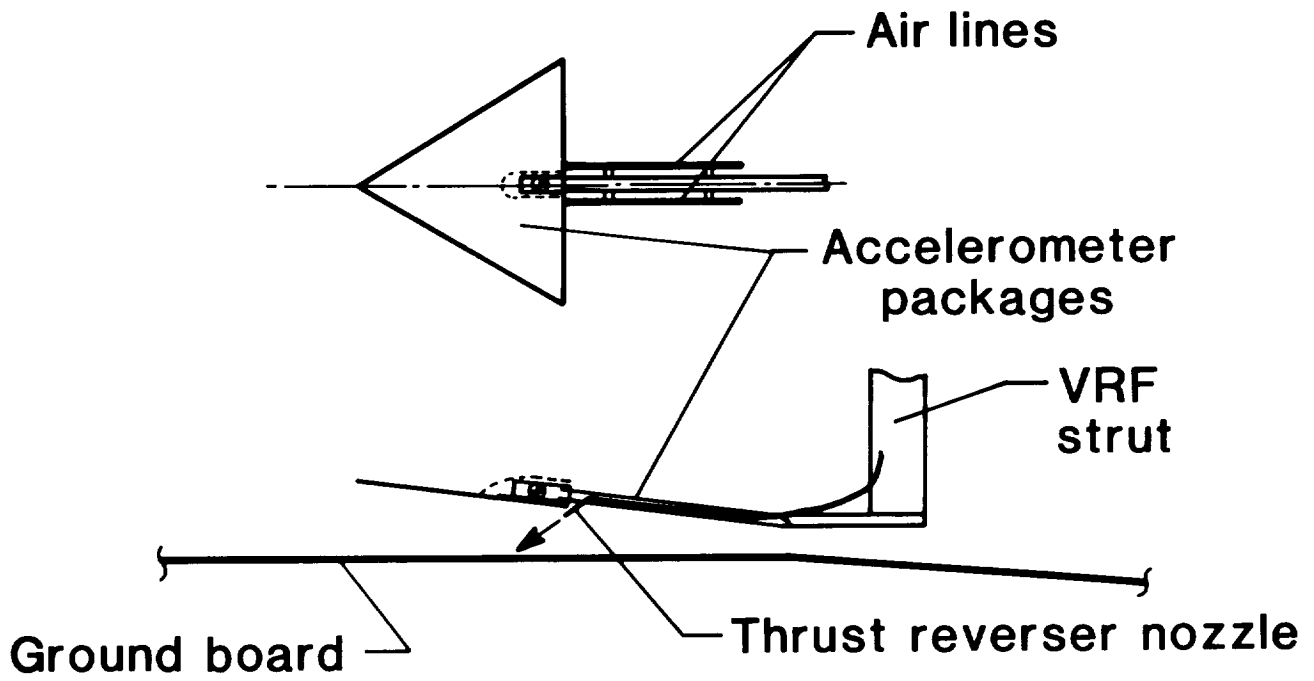
Figure 5. - Sketch of 60° delta wing model.
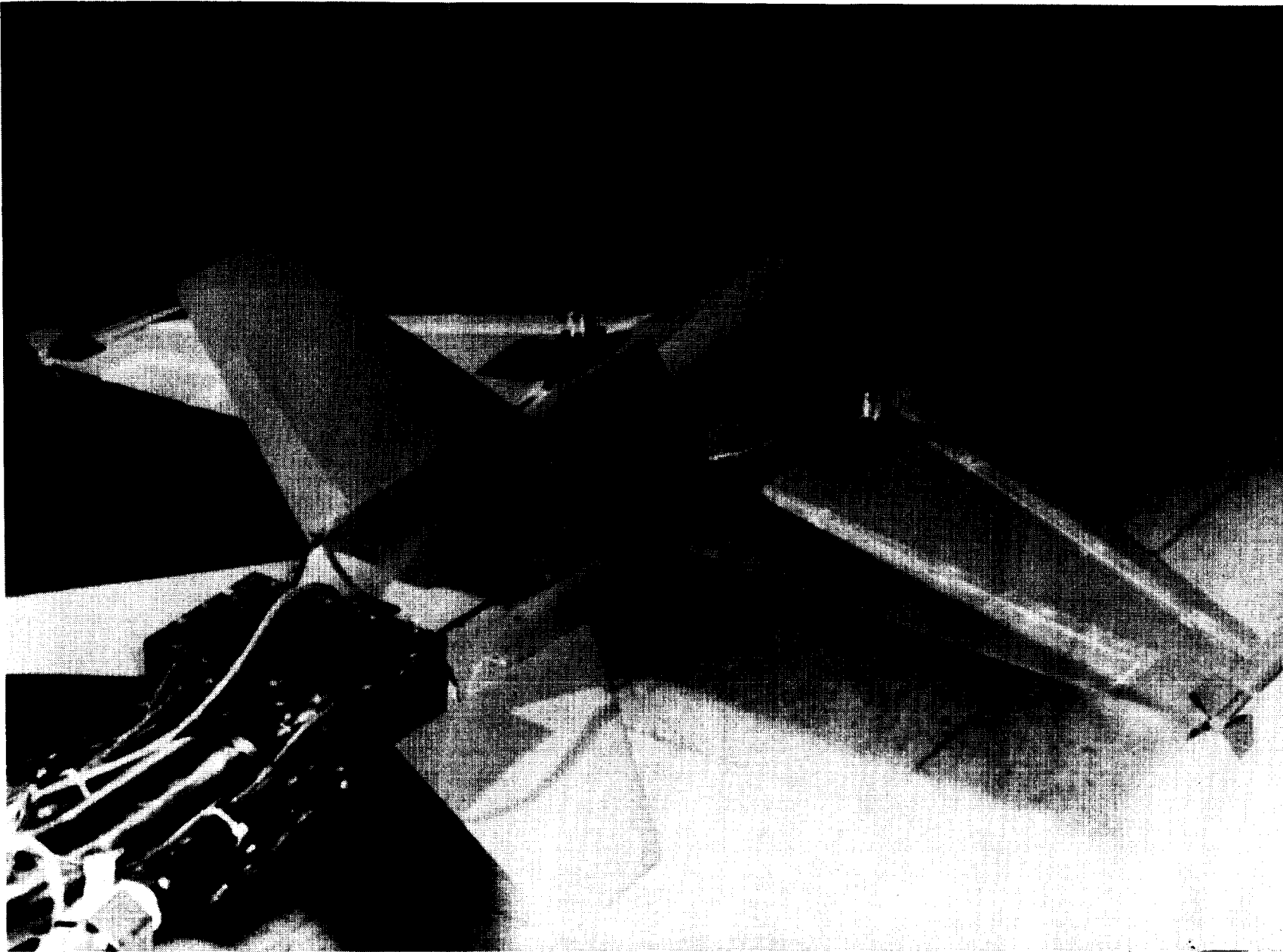
Figure 6. - Photograph of F-18 model.
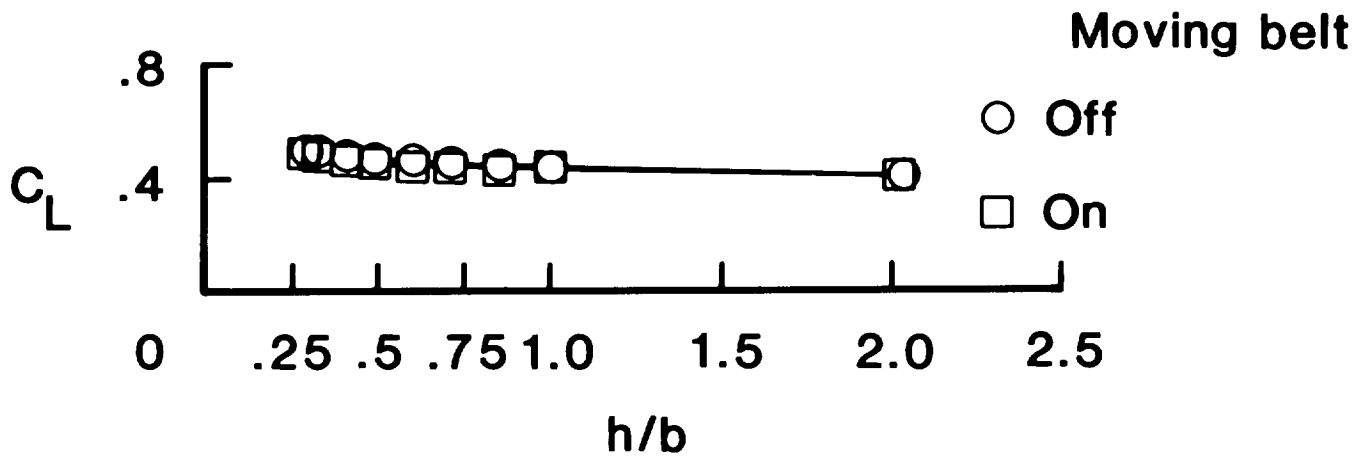
Figure 7. - Effect of moving belt ground plane on static ground effects of the 60° delta wing. α = 10 , NPR = 1.0, V∞ = 70 ft/sec and h = 0.
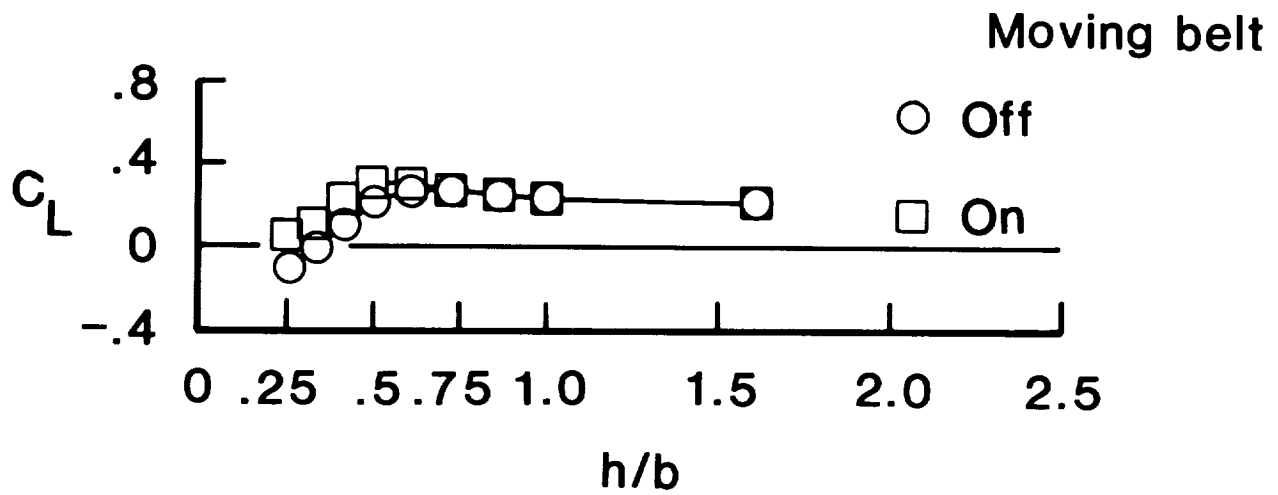
Figure 8. - Effect of moving belt ground plane on static ground effects of the 60° delta wing. $\alpha = 6.4°$, NPR $= 1.6$, $V_\infty = 70$ ft/sec and $\dot{h} = 0$.
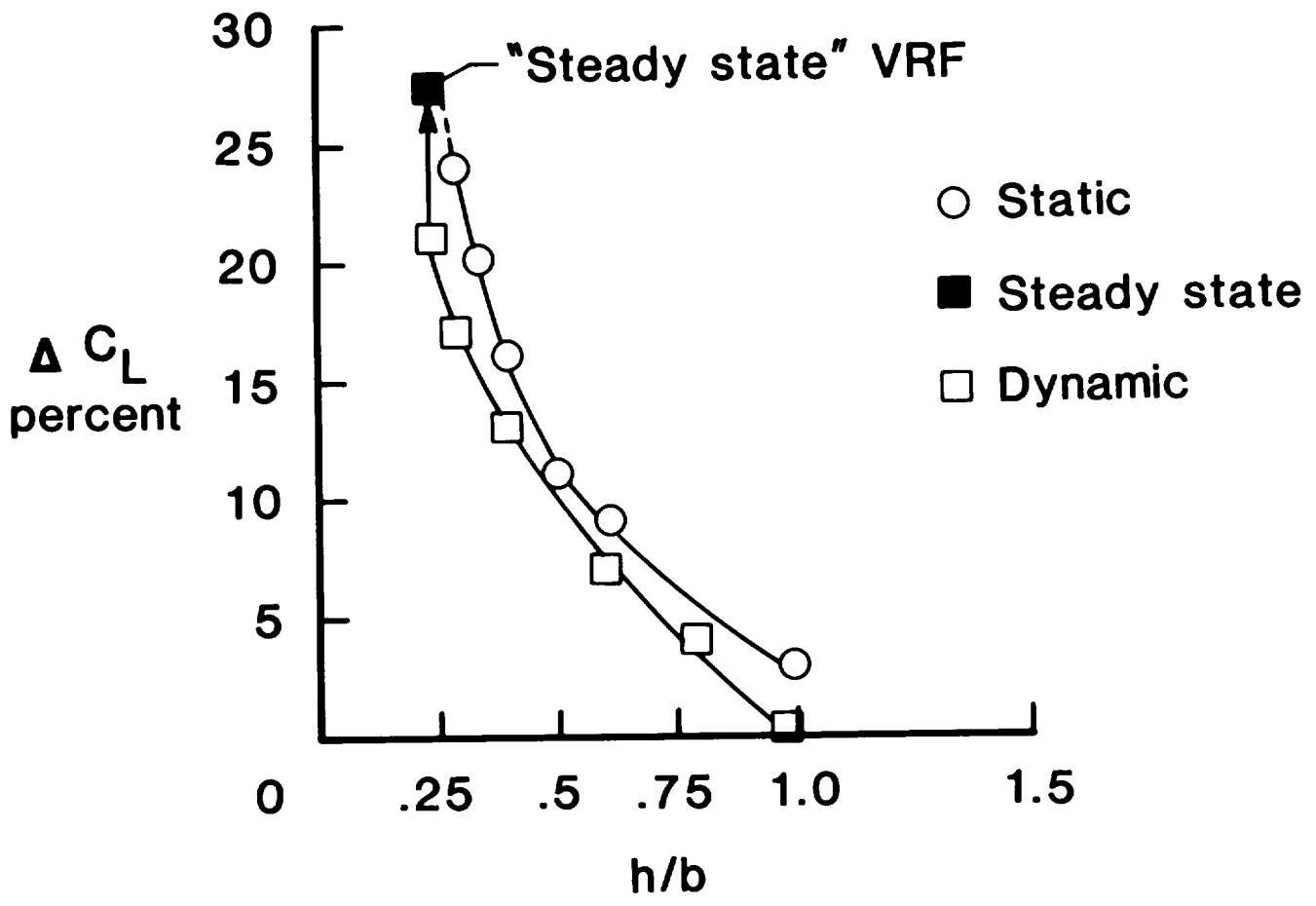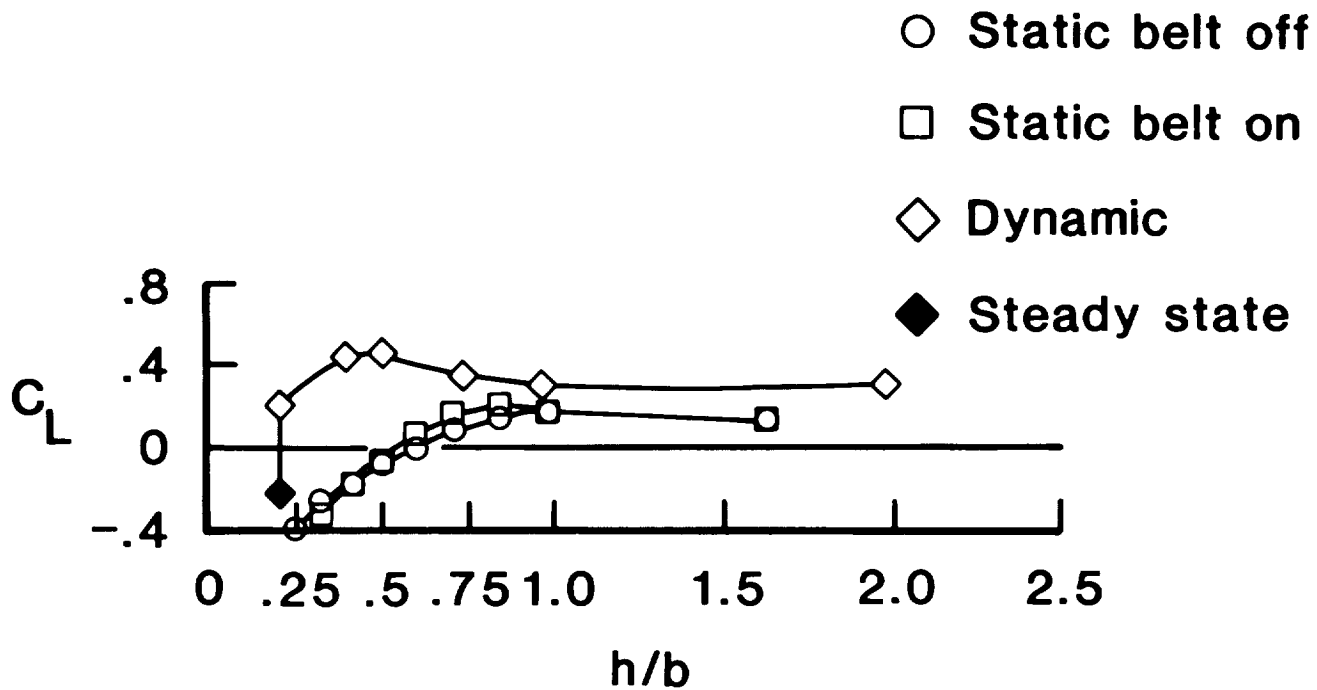
Figure 9. - Comparison of static and dynamic ground effects of the 60° delta wing. $\alpha = 10°$, NPR = 1.0, $V_\infty = 70$ ft/sec, and $\dot{h} = 4.9$ ft/sec.
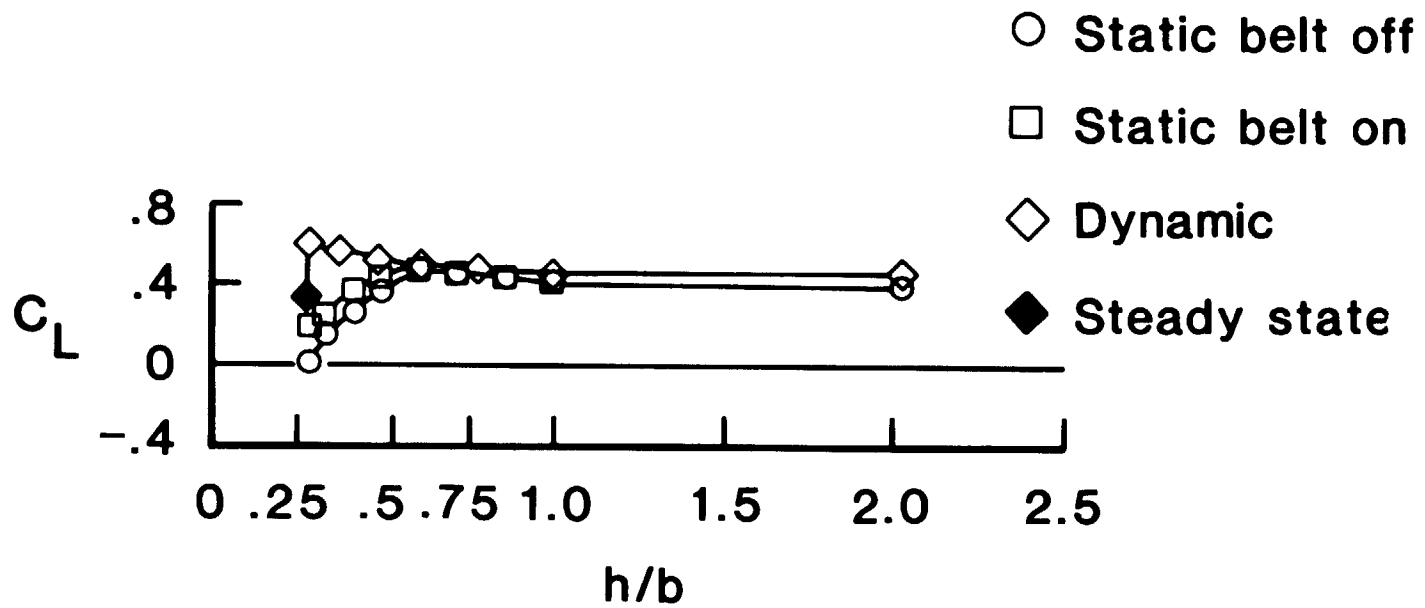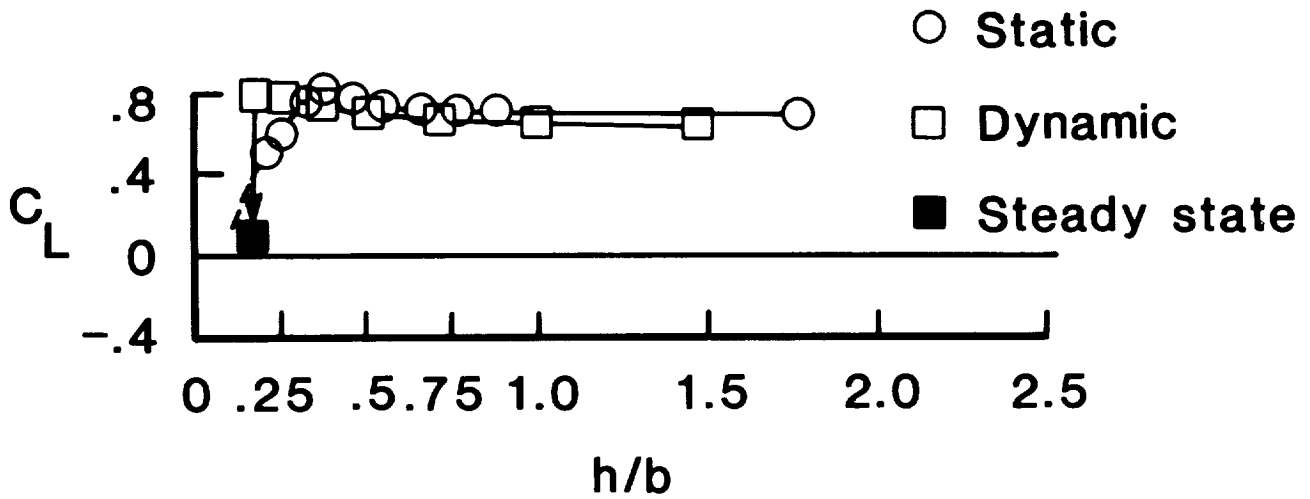
Figure 10. - Comparison of static and dynamic ground effects of the 60° delta wing.

$\alpha = 10°$, NPR = 1.6, $V_\infty = 90$ ft/sec, and $\dot{h} = 6.3$ ft/sec.

Figure 11. - Comparison of static and dynamic ground effects of the 60° delta wing. $\alpha = 6.4$, NPR = 1.8, $V_\infty = 70$ ft/sec and $\dot{h} = 4.9$ ft/sec.

Figure 12. - Comparison of static and dynamic ground effects of the F-18 configuration.

$\alpha = 8.4°$, NPR = 1.5, $\delta_f = 25°/20°/-10°$, Noz = $45°/0°$

$V_\infty = 99$ ft/sec and $\dot{h} = 6.9$ ft/sec.
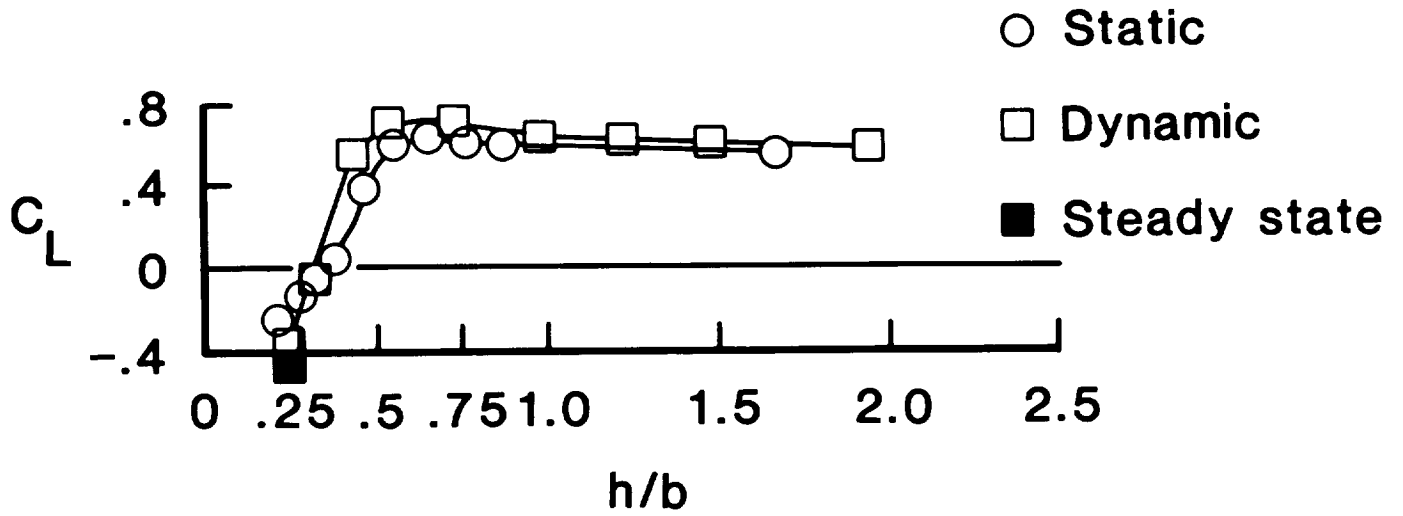
Figure 13. - Comparison of static and dynamic ground effects of the F-18 configuration.

$\alpha = 8.4°$, NPR = 2.5, $\delta_f = 25°/20°/-10°$, Noz = 45°/0°,
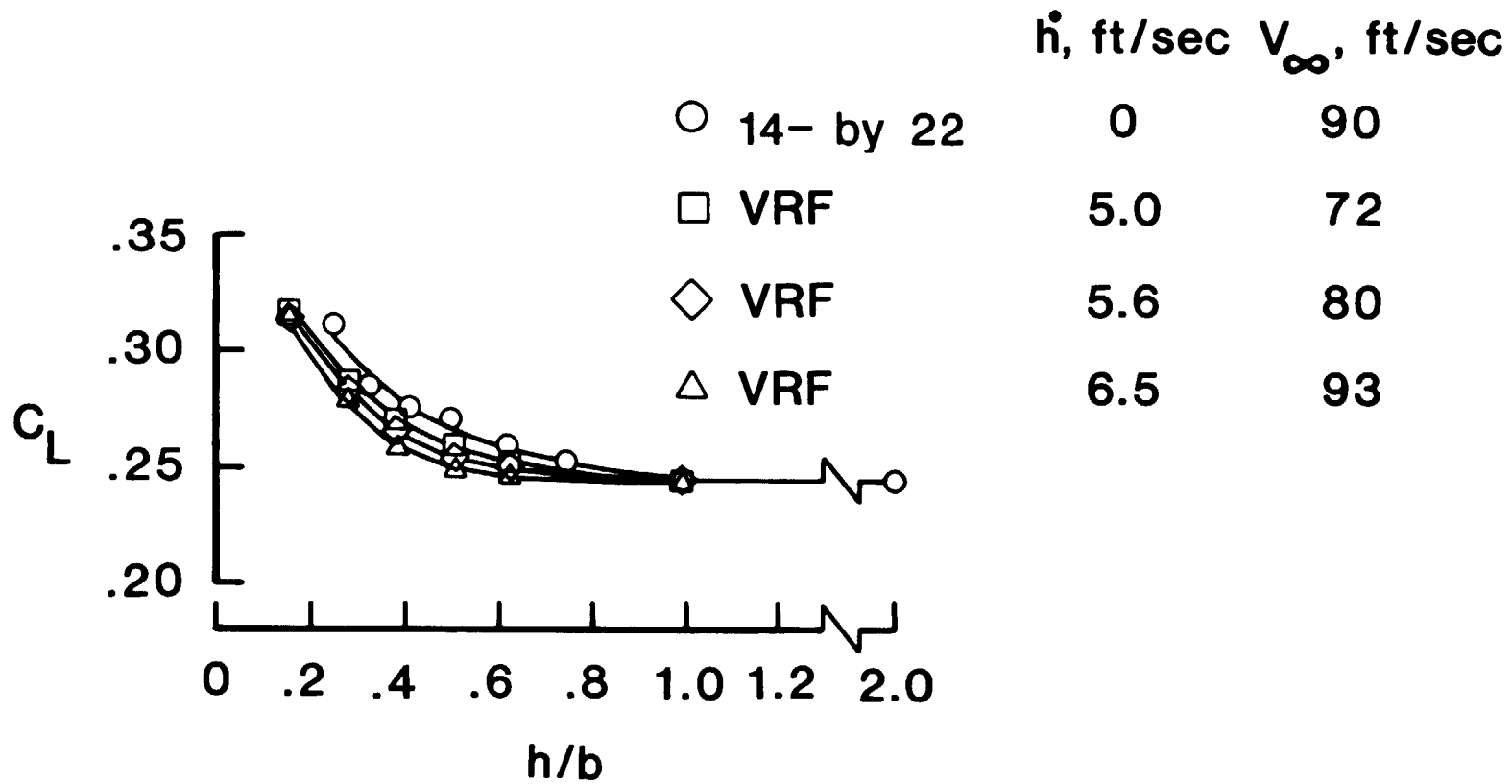
$V_\infty = 98$ ft/sec and $\dot{h} = 6.9$ ft/sec.

Figure 14. - Effect of rate-of-descent on dynamic ground effects of the 60° delta wing.

α = 6° and NPR = 1.0.